Iran J Sci Technol Trans Mech Eng (2019) 43 (Suppl 1):S641–S651
https://doi.org/10.1007/s40997-018-0185-6

RESEARCH PAPER

Vibration Analysis of Thick Functionally Graded Micro-plates Using HOSNDPT and Modified Couple Stress Theory

E. Mohseni[1] · A. R. Saidi[1] · M. Mohammadi[2]

Received: 16 May 2017 / Accepted: 9 May 2018 / Published online: 4 June 2018

Abstract
This paper develops a micro-scale vibration analysis of micro-plates using higher-order shear and normal deformable plate theory in conjunction with modified couple stress theory. The present model includes one material length scale parameter which takes into account the size effects. The equations of motions and boundary conditions are derived using Hamilton's principle. Analytical solutions for the free vibration problem of simply supported rectangular micro-plates are obtained. Numerical results are presented to illustrate the effect of small scale on the dynamic response of functionally graded micro-plates. The results show that the size-dependent effect increases the stiffness of the micro-plate and consequently increases the natural frequencies.

Keywords Functionally graded · Modified couple stress theory · Higher-order shear and normal deformable plate theory · Thick micro-plates

1 Introduction

Functionally graded materials (FGMs) are non-homogeneous composites that identify with their smooth and continuous variations in one or more directions. They are usually a combination of two different materials. Most popular FGMs are made of two components: one is metal and the other is ceramic. This combination is in order to achieve a composition with specific characteristics. FGMs have many advantages such as improved stress distribution, high thermal resistance, high toughness and reduced stress intensity factor. Recently, FGMs have found many applications in micro- and nano-scale devices and systems. Some of these applications are thin films (Fu et al. 2003; Lu et al. 2011), atomic force microscopes (AFMs) (Rahaeifard et al. 2009), micro- and nano-electromechanical systems (MEMS and NEMS) (Witvrouw and Mehta 2005; Lee et al. 2006) and so on. As the material size scales reduce to the micron scales, the stiffness and strength of materials increase because of material size effect. It is well known that classical continuum theories do not include the size effect in micro-scale structures. In order to overcome this deficiency, many higher-order theories such as classical couple stress theory with two material length scale parameters (Mindlin and Tiersten 1962; Toupin 1962; Koiter 1964), strain gradient theory with three material length scale parameters (Lam et al. 2003), micro-polar theory (Eringen 1967), non-local elasticity theory (Eringen 1972), surface elasticity (Gurtin et al. 1998) and modified couple stress theory with one material length scale parameter (Yang et al. 2002) have been developed to characterize the size effect in micro-scale structures. Based on the modified couple stress theory, many size-dependent beam and plate models have been developed to consider the size effects in small-scale structures. Park and Gao (2006) developed Euler–Bernoulli beam model for bending analysis of micro-beams. Ma et al. (2008) used Timoshenko beam model for micro-beams. Asghari et al. (2010) considered the Von-Karman nonlinear strains in the Timoshenko beam model. Euler–Bernoulli beam model for buckling analysis of axially loaded micro-beams was utilized by Akgöz and Civalek (2011). Their model was employed by Kong et al. (2008) and Kahrobaiyan et al.

✉ M. Mohammadi
meisam.mohammadi@vru.ac.ir

[1] Department of Mechanical Engineering, Shahid Bahonar University of Kerman, Kerman, Iran

[2] Department of Mechanical Engineering, Vali-e-Asr University of Rafsanjan, Rafsanjan, Iran

(2010) to study the vibration of micro-beams. Ke and Wang (2011) developed a Timoshenko beam model to study the size effect on dynamic stability of functionally graded (FG) micro-beams. Tsiatas (2009) first developed a Kirchhoff plate model (CPT) for static analysis of micro-plates. Yin et al. (2010) and Jomehzadeh et al. (2011) used the model presented by Tsiatas (2009) to study the vibration of micro-plates. This model was used by Akgöz and Civalek (2012) to study the vibration of nano-plates. Asghari and Taati (2013) dealt with classical (Kirchhoff) plate theory (CPT) of FG micro-plates. On the other hand, CPT does not consider shear deformation effect, so it provides accurate results for thin homogeneous plates only and is not suitable for thick plates. Using CPT for moderately thick plates leads to overestimation of results. Ma et al. (2011) and Ke et al. (2012) used the first-order shear deformation theory (FSDT) to develop a size-dependent model for accounting the shear deformation effects. In view of difficulties in determining shear correction factor, FSDT is not a convenient model, whereas it predicts sufficiently accurate results for moderately thick plates. Roque et al. (2013) used modified couple stress theory with meshless method to study the bending of simply supported isotropic micro-plates. Eshraghi et al. (2016) introduced solution methods capable of treating static bending and free vibration problems involving thermally loaded functionally graded annular and circular micro-plates using modified couple stress theory. Thai and Vo (2013) studied the static and dynamic behavior of functionally graded micro-plates. They used modified couple stress theory and sinusoidal shear deformation theory.

Behavior of thick structures in macro- and micro-scales was studied by some researchers (Arbind et al. 2014; Akgöz and Civalek 2015, 2017). Batra and Vidoli (2002) used virtual work principle to determine higher-order shear and normal deformable plate theory for thick plates with linear elastic incompressible anisotropic material. No shear correction factor was used, and vibration analysis of simply supported rectangular plates was investigated. The proposed higher-order shear and normal deformable plate theory is the closest theory to the three-dimensional elasticity solution. According to this theory, Legendre polynomials in thickness direction are used to approximate the displacement field components. Ghayesh et al. (2017) investigated the vibration analysis of geometrically imperfect three-layered shear deformable micro-beams. They considered both hardening and softening nonlinear behavior. Xiao et al. (2008) used meshless local Petrov–Galerkin method with radial basis function to study the static behavior of thick laminated composite elastic plates. They applied higher-order shear and normal deformable plate theory and considered different boundary conditions. Mohseni et al. (2017) studied the bending analysis of micro-plates based on the higher-order shear and normal deformable plate theory. They considered functionally graded distribution of material properties through the thickness.

In this paper, thick plates' model is developed for free vibration analysis of rectangular FG micro-plates using modified couple stress theory. Variational formulation based on Hamilton's principle is used in order to obtain the equations of motions and boundary conditions. A solution is determined for FG micro-plates with all edges simply supported (Navier solution). The natural frequencies are obtained for rectangular micro-plates with different material length scale parameters, various thickness ratios, various aspect ratios and some power law indices. The results indicate that the size length scale parameter has a significant effect when the thickness of the micro-plate becomes small.

2 Theoretical Formulation

2.1 Modified Couple Stress Theory

The modified couple stress theory which was proposed by Yang et al. (2002) is a modification of the classical couple stress theory. According to this theory, the virtual strain energy of a linear elastic micro-plate can be expressed as

$$\delta U = \int_V \left(\sigma_{ij}\delta\varepsilon_{ij} + m_{ij}\delta\chi_{ij}\right)\mathrm{d}V \tag{1}$$

where σ_{ij} are the Cartesian components of the stress tensor, ε_{ij} are the components of the strain tensor, m_{ij} are the components of deviatoric part of the symmetric couple stress tensor and χ_{ij} are the components of symmetric curvature tensor, so that

$$\chi_{ij} = \frac{1}{2}\left(\frac{\partial\theta_i}{\partial x_j} + \frac{\partial\theta_j}{\partial x_i}\right) \quad i,j = 1,2,3 \tag{2}$$

where θ_i are the components of rotation vector that in terms of displacement components are

$$\theta_1 = \frac{1}{2}\left(\frac{\partial u_3}{\partial x_2} - \frac{\partial u_2}{\partial x_3}\right) \tag{3a}$$

$$\theta_2 = \frac{1}{2}\left(\frac{\partial u_1}{\partial x_3} - \frac{\partial u_3}{\partial x_1}\right) \tag{3b}$$

$$\theta_3 = \frac{1}{2}\left(\frac{\partial u_2}{\partial x_1} - \frac{\partial u_1}{\partial x_2}\right) \tag{3c}$$

Also u_1, u_2 and u_3 are the Cartesian components of displacement field in x_1, x_2 and x_3 direction, respectively.

2.2 Kinematics

Consider a functionally graded (FG) micro-plate as shown in Fig. 1, where x_1x_2-plane coincides with the middle surface of the plate and the x_3-axis is perpendicular to this plane. As shown in Fig. 1, l_1 is the length of the plate along x_1 direction, l_2 is the width of the plate along x_2 direction and h is the thickness of the plate along x_3 direction. Using prescribed Cartesian coordinate, the infinitesimal deformations and displacement field of FG micro-plate based on the higher-order shear and normal deformable plate theory (HOSNDPT) are described as (Batra and Vidoli 2002)

$$u_i(x_1,x_2,x_3,t) = v_\alpha(x_1,x_2,x_3,t)\delta_{i\alpha} + w(x_1,x_2,x_3,t)\delta_{i3} \quad \alpha = 1,2 \tag{4}$$

where

$$v_\alpha(x_1,x_2,x_3,t) = L_a(x_3)v_\alpha^a(x_1,x_2,t) \tag{5a}$$

$$w(x_1,x_2,x_3,t) = L_a(x_3)w^a(x_1,x_2,t) \tag{5b}$$

and a = 0, 1, 2, …, k. Also, $L_a(x_3)$ are the orthonormal Legendre polynomials with the following properties as

$$L'_a(x_3) = D_{ab}L_b(x_3) \tag{6}$$

where $L'_a(x_3)$ is the first derivative of the orthonormal Legendre polynomial with respect to x_3.

Matrix D shows the matrix of differentiation coefficients. Hence, for k = 7, the general matrix D is defined as follows:

$$\begin{bmatrix} 0 & 0 & 0 & 0 & 0 & 0 & 0 & 0 \\ \sqrt{3} & 0 & 0 & 0 & 0 & 0 & 0 & 0 \\ 0 & \sqrt{15} & 0 & 0 & 0 & 0 & 0 & 0 \\ \sqrt{7} & 0 & \sqrt{35} & 0 & 0 & 0 & 0 & 0 \\ 0 & 3\sqrt{3} & 0 & 3\sqrt{7} & 0 & 0 & 0 & 0 \\ \sqrt{11} & 0 & \sqrt{35} & 0 & 3\sqrt{11} & 0 & 0 & 0 \\ 0 & \sqrt{39} & 0 & \sqrt{91} & 0 & \sqrt{143} & 0 & 0 \\ \sqrt{15} & 0 & 5\sqrt{3} & 0 & 3\sqrt{15} & 0 & \sqrt{195} & 0 \end{bmatrix} \tag{7}$$

According to Einstein's notation, repeated indices are summed even if they appear as a subscript and a superscript.

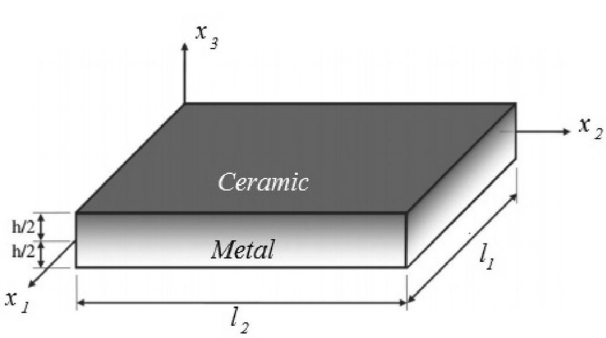

Fig. 1 Geometry of FG micro-plate

Hence, by considering the linear form of Von-Karman relations for strain–displacement equations, they are simplified as

$$\varepsilon_{ij} = \frac{1}{2}\left(u_{i,j} + u_{j,i}\right) \quad i,j = 1,2,3 \tag{8}$$

and also,

$$v_1 = L_a(x_3)v_1^a \tag{9a}$$

$$v_2 = L_a(x_3)v_2^a \tag{9b}$$

$$w = L_a(x_3)w^a \tag{9c}$$

2.3 Constitutive Relations

As explained earlier, it is assumed that the micro-plate is made of functionally graded materials where material properties are expressed by the power law function in the thickness direction as

$$\Gamma(x_3) = (\Gamma_c - \Gamma_m)\left(\frac{1}{2} + \frac{x_3}{h}\right)^N + \Gamma_m \tag{10}$$

In the above equation, Γ_c and Γ_m are the values of a typical material property, such as Young's modulus (E), density (ρ) or Lamè constants (λ, μ) of the ceramic and metal parts, respectively. In addition, N is the power law index denoting the volume fraction of the exponent. Constitutive relations for a linear elastic micro-plate in modified couple stress theory are

$$\sigma_{ij} = 2\mu\varepsilon_{ij} + \lambda\varepsilon_{kk}\delta_{ij} \tag{11}$$

$$\varepsilon_{kk} = \varepsilon_{11} + \varepsilon_{22} + \varepsilon_{33} \tag{12}$$

$$m_{ij} = 2\mu l^2\chi_{ij} \tag{13}$$

where ε_{kk} is the dilatation strain tensor and δ_{ij} is Kronecker delta. Also, Lamè constants, μ and λ in terms of engineering constants, are $\mu = \frac{E(x_3)}{2(1+v)}$ and $\lambda = \frac{E(x_3)v}{(1+v)(1-2v)}$. It must be noted that the Poisson's ratio (v) of FG micro-plate is considered to be constant due to its small variation through the thickness of the micro-plate. In Eq. (13), l is called the material length scale parameter which is regarded as a material property measuring the effect of couple stress. This parameter can be determined from torsion test of slim cylinder (Chong et al. 2001) or bending test of thin beams (Lam et al. 2003).

2.4 Equations of Motion

Hamilton's principle is used herein to derive the equations of motion and boundary conditions (Reddy 2002). Hence,

$$\int_0^T (\delta U + \delta W - \delta K)\mathrm{d}T = 0 \tag{14}$$

where U is the strain energy, W is the work done by external forces, K is the kinetic energy and T denotes time.

Using the variational approach, variation of strain energy δU is given by

$$\delta U=\int_{\Omega}\int_{-\frac{h}{2}}^{\frac{h}{2}}[(\sigma_{11}\delta\varepsilon_{11}+\sigma_{22}\delta\varepsilon_{22}+\sigma_{33}\delta\varepsilon_{33}+\sigma_{12}\delta\gamma_{12}+\sigma_{13}\delta\gamma_{13}+\sigma_{23}\delta\gamma_{23}) +(m_{11}\delta\chi_{11}+m_{22}\delta\chi_{22}+m_{33}\delta\chi_{33}+2m_{12}\delta\chi_{12}+2m_{13}\delta\chi_{13}+2m_{23}\delta\chi_{23})]\mathrm{d}x_1\mathrm{d}x_2\mathrm{d}x_3 \tag{15}$$

so that

$$\begin{aligned}\delta U=&\int_{\Omega}\int_{-\frac{h}{2}}^{\frac{h}{2}}\Big\{\Big[\sigma_{11}L_a(x_3)\delta v^a_{1,1}+\sigma_{22}L_a(x_3)\delta v^a_{2,2}+\sigma_{33}D_{ab}L_b(x_3)\delta w^a+\sigma_{12}\Big(L_a(x_3)\delta v^a_{1,2}+L_a(x_3)\delta v^a_{2,1}\Big)\\&+\sigma_{13}\Big(D_{ab}L_b(x_3)\delta v^a_1+L_a(x_3)\delta w^a_{,1}\Big)+\sigma_{23}\Big(D_{ab}L_b(x_3)\delta v^a_2+L_a(x_3)\delta w^a_{,2}\Big)\Big]+\Big[\frac{1}{2}m_{11}\Big(L_a(x_3)\delta w^a_{,12}\\&-D_{ab}L_b(x_3)\delta v^a_{2,1}\Big)+\frac{1}{2}m_{22}\Big(D_{ab}L_b(x_3)\delta v^a_{1,2}-L_a(x_3)\delta w^a_{,12}\Big)+\frac{1}{2}m_{33}\Big(D_{ab}L_b(x_3)\delta v^a_{2,12}\\&-D_{ab}L_b(x_3)\delta v^a_{1,2}\Big)+\frac{1}{2}m_{12}\Big(L_a(x_3)\delta w^a_{,22}-D_{ab}L_b(x_3)\delta v^a_{2,2}+D_{ab}L_b(x_3)\delta v^a_{1,1}-L_a(x_3)\delta w^a_{,11}\Big)\\&+\frac{1}{2}m_{13}\Big(D_{ab}L_b(x_3)\delta w^a_{,2}-D_{ab}D_{bc}L_c(x_3)\delta v^a_2+L_a(x_3)\delta v^a_{2,11}-L_a(x_3)\delta v^a_{1,12}\Big)\\&+\frac{1}{2}m_{23}\Big(D_{ab}D_{bc}L_c(x_3)\delta v^a_1-D_{ab}L_b(x_3)\delta w^a_{,1}-L_a(x_3)\delta v^a_{2,12}-L_a(x_3)\delta v^a_{1,22}\Big)\Big]\Big\}\mathrm{d}x_1\mathrm{d}x_2\mathrm{d}x_3\end{aligned} \tag{16}$$

Consider the following force and moment resultants:

$$M^a_{\alpha\beta}=\int_{-\frac{h}{2}}^{\frac{h}{2}}\sigma_{\alpha\beta}L_a(x_3)\mathrm{d}x_3 \tag{17a}$$

$$T^a_i=\int_{-\frac{h}{2}}^{\frac{h}{2}}\sigma_{i3}L_a(x_3)\mathrm{d}x_3 \tag{17b}$$

$$\mathcal{M}^a_{\alpha\beta}=\int_{-\frac{h}{2}}^{\frac{h}{2}}m_{\alpha\beta}L_a(x_3)\mathrm{d}x_3 \tag{17c}$$

$$\tau^a_i=\int_{-\frac{h}{2}}^{\frac{h}{2}}m_{i3}L_a(x_3)\mathrm{d}x_3 \tag{17d}$$

Substituting relations (17) in Eq. (16) and simplifying the results leads to

$$\begin{aligned}\delta U=&\int_{\Omega}\Big[\Big(M^a_{11}\delta v^a_{1,1}+M^a_{22}\delta v^a_{2,2}+T^b_{33}D_{ab}\delta w^a+M^a_{12}\delta v^a_{1,2}+M^a_{12}\delta v^a_{2,1}+T^b_1D_{ab}\delta v^a_1+T^a_1\delta w^a_{,1}+T^b_2D_{ab}\delta v^a_2\\&+T^b_2\delta w^a_{,2}\Big)+\frac{1}{2}\Big(\mathcal{M}^a_{11}\delta w^a_{,12}-\mathcal{M}^b_{11}D_{ab}\delta v^a_{2,1}+\mathcal{M}^b_{22}D_{ab}\delta v^a_{1,2}-\mathcal{M}^a_{22}\delta w^a_{,12}+\tau^b_3D_{ab}\delta v^a_{2,1}-\tau^b_3D_{ab}\delta v^a_{1,2}\\&+\mathcal{M}^a_{12}\delta w^a_{,22}-\mathcal{M}^b_{12}D_{ab}\delta v^a_{2,2}+\mathcal{M}^b_{12}D_{ab}\delta v^a_{1,1}-\mathcal{M}^a_{12}\delta w^a_{,11}+\tau^b_1D_{ab}\delta w^a_{,2}-\tau^c_1D_{ab}D_{bc}\delta v^a_2+\tau^a_1\delta v^a_{2,11}\\&-\tau^a_1\delta v^a_{1,12}+\tau^c_2D_{ab}D_{bc}\delta v^a_1-\tau^b_2D_{ab}\delta w^a_{,1}-\tau^a_2\delta v^a_{2,12}-\tau^a_2\delta v^a_{1,22}\Big)\Big]\mathrm{d}x_1\mathrm{d}x_2\mathrm{d}x_3\end{aligned} \tag{18}$$

Also, variation of the work done by external forces can be obtained as (Reddy and Kim 2012)

$$\begin{aligned}\delta W=&\int_V(\bar{f}_1\delta v_1+\bar{f}_2\delta v_2+\bar{f}_3\delta w+\bar{c}_1\delta\theta_1+\bar{c}_2\delta\theta_2+\bar{c}_3\delta\theta_3)\mathrm{d}x_1\mathrm{d}x_2\mathrm{d}x_3\\&+\int_{\Omega^+}(q^t_1\delta v_1+q^t_2\delta v_2+q^t_3\delta w)\mathrm{d}x_1\mathrm{d}x_2\\&+\int_{\Omega^-}(q^b_1\delta v_1+q^b_2\delta v_2+q^b_3\delta w)\mathrm{d}x_1\mathrm{d}x_2+\int_s(\bar{t}_1\delta v_1+\bar{t}_2\delta v_2+\bar{t}_3\delta w)\mathrm{d}s\end{aligned} \tag{19}$$

In Eq. (19), $\bar{f}_i$, $\bar{c}_i$, q_i and $\bar{t}_i\,(i=1,2,3)$ are body forces (per unit volume), body couples (per unit volume), distributed transverse loads on the plate surfaces (superscripts t and b indicate top and bottom) and surface forces, respectively. Also V, Ω and S denote the volume, surface and lateral surface of the micro-plate, respectively. Replacing Eqs. (9) in Eq. (19) leads to the following relation:

$$\begin{aligned}\delta W = \int\limits_{\Omega}\int\limits_{-h/2}^{h/2} & \left(\left(\bar{f}_1 L_a(x_3)\delta v_1^a + \bar{f}_2 L_a(x_3)\delta v_2^a + \bar{f}_3 L_a(x_3)\delta w^a\right) + \frac{1}{2}\bar{c}_1\left(L_a(x_3)\delta w_{,2}^a - D_{ab}L_b(x_3)\delta v_2^a\right)\right. \\ & + \frac{1}{2}\bar{c}_2\left(D_{ab}L_b(x_3)\delta v_1^a - L_a(x_3)\delta w_{,1}^a\right) + \left.\frac{1}{2}\bar{c}_3\left(L_a(x_3)\delta v_{2,1}^a - L_a(x_3)\delta v_{1,2}^a\right)\right)\mathrm{d}x_1\mathrm{d}x_2\mathrm{d}x_3 \\ & + \int_{\Omega}\left(q_1^t L_a\left(\frac{h}{2}\right)\delta v_1^a + q_2^t L_a\left(\frac{h}{2}\right)\delta v_2^a + q_3^t L_a\left(\frac{h}{2}\right)\delta w^a + q_1^b L_a\left(-\frac{h}{2}\right)\delta v_1^a + q_2^b L_a\left(-\frac{h}{2}\right)\delta v_2^a\right. \\ & \left. + q_3^b L_a\left(-\frac{h}{2}\right)\delta w^a\right)\mathrm{d}x_1\mathrm{d}x_2 + \int_s\left(\bar{t}_1 L_a(x_3)\delta v_1^a + \bar{t}_2 L_a(x_3)\delta v_2^a + \bar{t}_3 L_a(x_3)\delta w^a\right)\mathrm{d}s\end{aligned} \tag{20}$$

so that

$$\begin{aligned}\delta W = \int_{\Omega} & \left(F_1^a\delta v_1^a + F_2^a\delta v_2^a + F_3^a\delta w^a + \frac{1}{2}c_1^a\delta w_{,2}^a - \frac{1}{2}c_1^b D_{ab}\delta v_2^a\right. \\ & \left. + \frac{1}{2}c_2^b D_{ab}\delta v_1^a - \frac{1}{2}c_2^a\delta w_{,1}^a + \frac{1}{2}c_3^a\delta v_{2,1}^a - \frac{1}{2}c_3^a\delta v_{1,2}^a\right)\mathrm{d}x_1\mathrm{d}x_2 \\ & + \int_s\left(t_1^a\delta v_1^a + t_2^a\delta v_2^a + t_3^a\delta w^a\right)\mathrm{d}s\end{aligned} \tag{21}$$

It should be noted that variation of work done by the external forces is simplified using Reddy's definitions (Reddy and Kim 2012) as

$$f_i^a = \int_{-\frac{h}{2}}^{\frac{h}{2}} L_a(x_3)\bar{f}_i\mathrm{d}x_3 \tag{22a}$$

$$t_i^a = \int_{-\frac{h}{2}}^{\frac{h}{2}} L_a(x_3)\bar{t}_i\mathrm{d}x_3 \tag{22b}$$

$$c_i^a = \int_{-\frac{h}{2}}^{\frac{h}{2}} L_a(x_3)\bar{c}_i\mathrm{d}x_3 \tag{22c}$$

$$F_i^a = q_i^t L_a\left(\frac{h}{2}\right) + q_i^b L_a\left(-\frac{h}{2}\right) + f_i^a \tag{22d}$$

Also, variation of kinetic energy is expressed as

$$\delta K = \int_{\Omega}\int_{-\frac{h}{2}}^{\frac{h}{2}}\rho\left(\frac{\partial v_1}{\partial t}\frac{\partial\delta v_1}{\partial t} + \frac{\partial v_2}{\partial t}\frac{\partial\delta v_2}{\partial t} + \frac{\partial w}{\partial t}\frac{\partial\delta w}{\partial t}\right)\mathrm{d}x_1\mathrm{d}x_2\mathrm{d}x_3 \tag{23}$$

Replacing Eqs. (9) in Eq. (23) and simplifying the relations results in

$$\begin{aligned}\delta K = \int_{\Omega}\int_{-\frac{h}{2}}^{\frac{h}{2}}\rho & \left(L_a(x_3)\dot{v}_1^a L_b(x_3)\delta\dot{v}_1^b + L_a(x_3)\dot{v}_2^a L_b(x_3)\delta\dot{v}_2^b\right. \\ & \left. + L_a(x_3)w_1^a L_b(x_3)\delta w_1^b\right)\mathrm{d}x\cdot\mathrm{d}x_2\mathrm{d}x_3\end{aligned} \tag{24}$$

Let

$$R_{ab} = R_{ba} = \int_{-\frac{h}{2}}^{\frac{h}{2}}\rho L_a(x_3)L_b(x_3)\mathrm{d}x_3 \tag{25}$$

Therefore, Eq. (24) is simplified as

$$\delta K = \int_{\Omega} R_{ab}\left(\dot{v}_1^a\delta\dot{v}_1^b + \dot{v}_2^a\delta\dot{v}_2^b + \dot{w}^a\delta\dot{w}^b\right)\mathrm{d}x_1\mathrm{d}x_2 \tag{26}$$

By substituting Eqs. (18), (21) and (26) into Eq. (14) and integrating by parts, the following equations of motion for FG micro-plates based on the HOSNDPT and modified couple stress theory are determined:

$$\begin{aligned}\delta v_1^a : & \left(R_{ba}\ddot{v}_1^b + T_1^b D_{ab} + \frac{1}{2}\tau_2^c D_{ab}D_{bc} + F_1^a + \frac{1}{2}c_2^b D_{ab}\right. \\ & - \frac{\partial M_{11}^a}{\partial x_1} - \frac{1}{2}\frac{\partial \mathcal{M}_{12}^b}{\partial x_1}D_{ab} - \frac{\partial M_{12}^a}{\partial x_2} - \frac{1}{2}\frac{\partial \mathcal{M}_{22}^b}{\partial x_2}D_{ab} \\ & \left. + \frac{1}{2}\frac{\partial\tau_3^b}{\partial x_2}D_{ab} + \frac{1}{2}\frac{\partial c_3^a}{\partial x_2} - \frac{1}{2}\frac{\partial}{\partial x_2}\left(\frac{\partial\tau_1^a}{\partial x_1}\right) - \frac{1}{2}\frac{\partial}{\partial x_2}\left(\frac{\partial\tau_2^a}{\partial x_2}\right)\right) = 0\end{aligned} \tag{27a}$$

$$\begin{aligned}\delta v_2^a : & \left(R_{ba}\ddot{v}_2^b + T_2^b D_{ab} - \frac{1}{2}\tau_1^c D_{ab}D_{bc} + F_2^a - \frac{1}{2}c_1^b D_{ab}\right. \\ & - \frac{\partial M_{12}^a}{\partial x_1} + \frac{1}{2}\frac{\partial \mathcal{M}_{11}^b}{\partial x_1}D_{ab} - \frac{\partial M_{22}^a}{\partial x_2} + \frac{1}{2}\frac{\partial \mathcal{M}_{12}^b}{\partial x_2}D_{ab} \\ & \left. - \frac{1}{2}\frac{\partial\tau_3^b}{\partial x_1}D_{ab} - \frac{1}{2}\frac{\partial c_3^a}{\partial x_1} + \frac{1}{2}\frac{\partial}{\partial x_1}\left(\frac{\partial\tau_1^a}{\partial x_1}\right) + \frac{1}{2}\frac{\partial}{\partial x_2}\left(\frac{\partial\tau_2^a}{\partial x_1}\right)\right) = 0\end{aligned} \tag{27b}$$

$$\begin{aligned}\delta w^a : & \left(R_{ba}\ddot{w}^b + T_3^b D_{ab} + F_3^a + \frac{1}{2}\frac{\partial\tau_2^b}{\partial x_1}D_{ab} - \frac{1}{2}\frac{\partial\tau_1^b}{\partial x_2}D_{ab}\right. \\ & + \frac{1}{2}\frac{\partial c_2^a}{\partial x_1} - \frac{1}{2}\frac{\partial c_1^a}{\partial x_2} - \frac{\partial T_1^a}{\partial x_1} - \frac{\partial T_2^a}{\partial x_2} - \frac{1}{2}\frac{\partial}{\partial x_1}\left(\frac{\partial \mathcal{M}_{12}^a}{\partial x_1}\right) \\ & \left. + \frac{1}{2}\frac{\partial}{\partial x_2}\left(\frac{\partial \mathcal{M}_{11}^a}{\partial x_1}\right) - \frac{1}{2}\frac{\partial}{\partial x_2}\left(\frac{\partial \mathcal{M}_{22}^a}{\partial x_1}\right) + \frac{1}{2}\frac{\partial}{\partial x_2}\left(\frac{\partial \mathcal{M}_{12}^a}{\partial x_2}\right)\right) = 0\end{aligned} \tag{27c}$$

For an FG micro-plate without body forces, body couples and surface tractions, equations of motion are reduced to

$$\delta v_1^a:\left(R_{ba}\ddot{v}_1^b+T_1^bD_{ab}+\frac{1}{2}\tau_2^cD_{ab}D_{bc}-\frac{\partial M_{11}^a}{\partial x_1}-\frac{1}{2}\frac{\partial\mathcal{M}_{12}^b}{\partial x_1}D_{ab}-\frac{\partial M_{12}^a}{\partial x_2}-\frac{1}{2}\frac{\partial\mathcal{M}_{22}^b}{\partial x_2}D_{ab}+\frac{1}{2}\frac{\partial\tau_3^b}{\partial x_2}D_{ab}-\frac{1}{2}\frac{\partial}{\partial x_2}\left(\frac{\partial\tau_1^a}{\partial x_1}\right)-\frac{1}{2}\frac{\partial}{\partial x_2}\left(\frac{\partial\tau_2^a}{\partial x_2}\right)\right)=0 \tag{28a}$$

$$\delta v_2^a:\left(R_{ba}\ddot{v}_2^b+T_2^bD_{ab}-\frac{1}{2}\tau_1^cD_{ab}D_{bc}-\frac{\partial M_{12}^a}{\partial x_1}+\frac{1}{2}\frac{\partial\mathcal{M}_{11}^b}{\partial x_1}D_{ab}-\frac{\partial M_{22}^a}{\partial x_2}+\frac{1}{2}\frac{\partial\mathcal{M}_{12}^b}{\partial x_2}D_{ab}-\frac{1}{2}\frac{\partial\tau_3^b}{\partial x_1}D_{ab}+\frac{1}{2}\frac{\partial}{\partial x_1}\left(\frac{\partial\tau_1^a}{\partial x_1}\right)+\frac{1}{2}\frac{\partial}{\partial x_2}\left(\frac{\partial\tau_2^a}{\partial x_1}\right)\right)=0 \tag{28b}$$

$$\delta w^a:\left(R_{ba}\ddot{w}^b+T_3^bD_{ab}+\frac{1}{2}\frac{\partial\tau_2^b}{\partial x_1}D_{ab}-\frac{1}{2}\frac{\partial\tau_1^b}{\partial x_2}D_{ab}-\frac{\partial T_1^a}{\partial x_1}-\frac{\partial T_2^a}{\partial x_2}-\frac{1}{2}\frac{\partial}{\partial x_1}\left(\frac{\partial\mathcal{M}_{12}^a}{\partial x_1}\right)+\frac{1}{2}\frac{\partial}{\partial x_2}\left(\frac{\partial\mathcal{M}_{11}^a}{\partial x_1}\right)-\frac{1}{2}\frac{\partial}{\partial x_2}\left(\frac{\partial\mathcal{M}_{22}^a}{\partial x_1}\right)+\frac{1}{2}\frac{\partial}{\partial x_2}\left(\frac{\partial\mathcal{M}_{12}^a}{\partial x_2}\right)\right)=0 \tag{28c}$$

Using the variational approach and Hamilton's principle, boundary conditions are derived besides the equations of motion. Hence, they are

$$\left(t_1^a+\left(M_{11}^a+\frac{1}{2}\mathcal{M}_{12}^bD_{ab}+\frac{1}{2}\frac{\partial\tau_1^a}{\partial x_1}\right)n_1+\left(M_{12}^a+\frac{1}{2}\mathcal{M}_{22}^bD_{ab}-\frac{1}{2}\tau_3^bD_{ab}-\frac{1}{2}c_3^a+\frac{1}{2}\frac{\partial\tau_2^a}{\partial x_2}\right)n_2\right)=0 \tag{29a}$$

$$\left(t_2^a+\left(M_{12}^a-\frac{1}{2}\mathcal{M}_{11}^bD_{ab}+\frac{1}{2}\tau_3^bD_{ab}+\frac{1}{2}c_3^a-\frac{1}{2}\frac{\partial\tau_1^a}{\partial x_1}\right)\mathbf{n}_1+\left(M_{22}^a-\frac{1}{2}\mathcal{M}_{12}^bD_{ab}-\frac{1}{2}\frac{\partial\tau_2^a}{\partial x_2}\right)\mathbf{n}_2\right)=0 \tag{29b}$$

$$\left(t_3^a+\left(T_1^a-\frac{1}{2}\tau_2^bD_{ab}-\frac{1}{2}c_2^a+\frac{1}{2}\frac{\partial\mathcal{M}_{12}^a}{\partial x_1}\right)\mathbf{n}_1\right)+\left(T_2^a+\frac{1}{2}\tau_1^bD_{ab}+\frac{1}{2}c_1^a-\frac{1}{2}\frac{\partial\mathcal{M}_{11}^a}{\partial x_1}+\frac{1}{2}\frac{\partial\mathcal{M}_{22}^a}{\partial x_1}-\frac{1}{2}\frac{\partial\mathcal{M}_{12}^a}{\partial x_2}\right)\mathbf{n}_2=0 \tag{29c}$$

where $(\mathbf{n}_1,\mathbf{n}_2,\mathbf{n}_3)$ are unit outward normal vectors in (x_1, x_2, x_3) directions, respectively.

Clearly, when the size effects are neglected, i.e., $l = 0$, the present model is reduced to the relations for FG plate shown by Sheikholeslami and Saidi (2013).

Further, considering harmonic motion, the solutions of Eqs. (28) are assumed as

$$v_\alpha^a(x_1,x_2,t)=e^{i\omega t}V_\alpha^a(x_1,x_2) \tag{30a}$$

$$w^a(x_1,x_2,t)=e^{i\omega t}W^a(x_1,x_2) \tag{30b}$$

where $i=\sqrt{-1}$ and ω is the frequency of motion.

Replacing Eqs. (30) in Eqs. (28), system homogenous equations are determined where the Eigen values are the natural frequency.

2.5 Analytical Solutions

In this section, an analytical solution for free vibration of simply supported rectangular micro-plates is presented. Based on the Navier approach, the displacement components are approximated using double series solution as

$$V_1^a(x_1,x_2)=\sum_{m,n=0}^{\infty}\tilde{V}_1^{amn}\cos\left(\frac{m\pi x_1}{l_1}\right)\sin\left(\frac{n\pi x_2}{l_2}\right) \tag{31a}$$

Table 1 Comparison of dimensionless natural frequency $\bar{\omega}$ for square homogeneous micro-plate

l/h	l_1/h = 5			l_1/h = 20			l_1/h = 100		
	Present study	Yin et al. (2010)	Diff. %	Present study	Yin et al. (2010)	Diff. %	Present study	Yin et al. (2010)	Diff. %
0	5.3036	5.9734	11.21	5.9219	5.9734	0.82	5.9713	5.9734	0.04
0.2	5.7561	6.4556	10.84	6.4016	6.4556	0.84	6.4535	6.4556	0.03
0.4	6.8966	7.7239	10.71	7.6587	7.7239	0.84	7.7213	7.7239	0.03
0.6	8.3932	9.4673	11.35	9.3801	9.4673	0.92	9.4638	9.4673	0.04
0.8	10.0214	11.4713	12.64	11.3494	11.4713	1.06	11.4663	11.4713	0.04
1	11.6544	13.6213	14.44	13.4498	13.6213	1.26	13.6143	13.6213	0.05

Table 2 Comparison of dimensionless natural frequency $\bar{\omega}$ for square homogeneous micro-plate

l/h	$l_1/h = 5$			$l_1/h = 20$			$l_1/h = 100$		
	Present study	Thai and Kim (2013)	Diff. %	Present study	Thai and Kim (2013)	Diff. %	Present study	Thai and Kim (2013)	Diff. %
0	5.3036	5.2813	0.42	5.9219	5.9199	0.03	5.9713	5.9712	0.00
0.2	5.7561	5.7699	− 0.24	6.4016	6.4207	− 0.30	6.4535	6.4535	0.00
0.4	6.8966	7.0330	− 1.98	7.6587	7.6708	− 0.16	7.7213	7.7217	− 0.01
0.6	8.3932	8.7389	− 4.12	9.3801	9.4116	− 0.34	9.4638	9.4651	− 0.01
0.8	10.0214	10.6766	− 6.54	11.3494	11.4108	− 0.54	11.4663	11.4689	− 0.02
1	11.6544	12.7408	− 9.32	13.4498	13.5545	− 0.78	13.6186	13.6189	− 0.03

Table 3 Comparison of dimensionless natural frequency $\bar{\omega}$ for square FG micro-plate

l_1/h	l/h	$N = 0.5$			$N = 1$			$N = 2$		
		Present study	Thai and Kim (2013)	Diff. %	Present study	Thai and Kim (2013)	Diff. %	Present study	Thai and Kim (2013)	Diff. %
5	0	4.5394	4.5180	0.47	4.0989	4.0781	0.51	3.6961	3.6805	0.42
	0.2	4.9671	4.9715	− 0.09	4.5078	4.5094	− 0.04	4.0697	4.0755	− 0.14
	0.4	6.0373	6.1339	− 1.60	5.5234	5.6071	− 1.52	4.9905	5.0763	− 1.72
	0.6	7.4255	7.6895	− 3.56	6.8307	7.0662	− 3.45	6.1705	6.4011	− 3.74
	0.8	8.9221	9.4456	− 5.87	8.2331	8.7058	− 5.74	7.4348	7.8861	− 6.07
	1	10.4138	11.3086	− 8.59	9.6263	10.4397	− 8.45	8.6907	9.4536	− 8.78
10	0	4.9074	4.9014	0.07	4.4258	4.4192	0.15	4.0136	4.0090	0.11
	0.2	5.3558	5.3571	− 0.02	4.8520	4.8526	− 0.01	4.3983	4.4006	− 0.52
	0.4	6.5048	6.5361	− 0.48	5.9393	5.9664	− 0.46	5.3787	5.4071	− 0.53
	0.6	8.0421	8.1295	− 1.09	7.3841	7.4619	− 1.05	6.6811	6.7580	− 1.15
	0.8	9.7361	9.9368	− 1.81	8.9943	9.1537	− 1.77	8.1330	8.2863	− 1.88
	1	11.5596	11.8682	− 2.67	10.6706	10.9511	− 2.63	9.6451	9.9101	− 2.75
20	0	5.0198	5.0180	0.04	4.5245	4.5228	0.04	4.1113	4.1100	0.03
	0.2	5.4740	5.4744	− 0.01	4.9566	4.9566	0.00	4.4999	4.5006	− 0.02
	0.4	6.6500	6.6585	− 0.13	6.0682	6.0756	− 0.12	5.5004	5.5082	− 0.14
	0.6	8.2393	8.2630	− 0.29	7.5606	7.5817	− 0.28	6.8451	6.8661	− 0.31
	0.8	10.0410	10.0895	− 0.48	9.2450	9.2887	− 0.47	8.3640	8.4062	− 0.50
	1	11.9517	12.0372	− 0.72	11.0266	11.1042	− 0.71	9.9715	10.0450	− 0.74
100	0	5.0576	5.0575	0.00	4.5580	4.5579	0.00	4.1445	4.1445	0.00
	0.2	5.5142	5.5142	0.00	4.9922	4.9922	0.00	4.5346	4.5346	0.00
	0.4	6.6996	6.7000	− 0.01	6.1123	6.1126	0.00	5.5422	5.5425	− 0.01
	0.6	8.3074	8.3084	− 0.01	7.6215	7.6224	− 0.01	6.9019	6.9027	− 0.01
	0.8	10.1382	10.1402	− 0.02	9.3326	9.3344	− 0.02	8.4450	8.4467	− 0.02
	1	12.0908	12.0944	− 0.03	11.1528	11.1560	− 0.03	10.0874	10.0904	− 0.03

$$V_2^a(x_1, x_2) = \sum_{m,n=0}^{\infty} \tilde{V}_2^{amn} \sin\left(\frac{m\pi x_1}{l_1}\right) \cos\left(\frac{n\pi x_2}{l_2}\right) \tag{31b}$$

$$W^a(x_1, x_2) = \sum_{m,n=0}^{\infty} \tilde{W}^{amn} sin\left(\frac{m\pi x_1}{l_1}\right) sin\left(\frac{n\pi x_2}{l_2}\right) \tag{31c}$$

where m and n are integers that show the mode numbers and $(\tilde{V}_1^{amn}, \tilde{V}_2^{amn}, \tilde{W}^{amn})$ are coefficients of the components of the displacement field.

According to the Navier solution, the components of the displacement field are extended using double trigonometric

Table 4 Convergence of natural frequency $\bar{\omega}$ versus variation of Legendre polynomial order

l_1/h	l/h	Legendre polynomial order, k				
		1	2	3	4	5
5	0	5.8338	5.3576	5.3042	5.3036	5.3036
	0.2	6.2262	5.7947	5.7581	5.7579	5.7561
	0.4	7.2569	6.9202	6.8982	6.8981	6.8966
	0.6	8.6527	8.4096	8.3939	8.3938	8.3932
	0.8	10.2015	10.0340	10.0216	10.0216	10.0214
	1	11.7747	11.6644	11.6545	11.6545	11.6544
10	0	6.3820	5.7950	5.7770	5.7769	5.7769
	0.2	6.8055	6.2628	6.2502	6.2502	6.2495
	0.4	7.9343	7.4851	7.4771	7.4771	7.4765
	0.6	9.5025	9.1456	9.1393	9.1393	9.1389
	0.8	11.3045	11.0226	11.0169	0.0169	11.0167
	1	13.2172	12.9937	12.9882	12.9882	12.9881
30	0	6.5843	5.9525	5.9503	5.9503	5.9503
	0.2	7.0212	6.4331	6.4315	6.4315	6.4314
	0.4	8.1924	7.6957	7.6947	7.6947	7.6946
	0.6	9.8367	9.4290	9.4282	9.4282	9.4281
	0.8	11.7540	11.4172	11.4164	11.4164	11.4164
	1	13.8274	13.5447	13.5439	13.5439	13.5439
100	0	6.6088	5.9715	5.9713	5.9713	5.9713
	0.2	7.0475	6.4536	6.4535	6.4535	6.4535
	0.4	8.2240	7.7213	7.7213	7.7213	7.7212
	0.6	9.8781	9.4639	9.4638	9.4638	9.4638
	0.8	11.8104	11.4664	11.4664	11.4664	11.4663
	1	13.9051	13.6144	13.6143	13.6143	13.6143

Table 5 Dimensionless natural frequency $\bar{\omega}$ of square FG micro-plate

l_1/h	l/h	Power law index, N				
		0.5	1	2	5	10
5	0	4.5394	4.0989	3.6961	3.4047	3.2643
	0.2	4.9671	4.5078	4.0697	3.7141	3.5335
	0.4	6.0373	5.5234	4.9905	4.4700	4.1898
	0.6	7.4255	6.8307	6.1705	5.4443	5.0459
	0.8	8.9221	8.2331	7.4348	6.4982	5.9812
	1	10.4138	9.6263	8.6907	7.5536	6.9245
10	0	4.9074	4.4258	4.0136	3.7716	3.6414
	0.2	5.3558	4.8520	4.3983	4.0808	3.9087
	0.4	6.5048	5.9393	5.3787	4.8772	4.6020
	0.6	8.0421	7.3841	6.6811	5.9528	5.5502
	0.8	9.7631	8.9943	8.1330	7.1674	6.6312
	1	11.5596	10.6706	9.6451	8.4430	7.7738
20	0	5.0198	4.5245	4.1113	3.8893	3.7635
	0.2	5.4740	4.9566	4.4999	4.1986	4.0302
	0.4	6.6500	6.0682	5.5004	5.0090	4.7366
	0.6	8.2393	7.5606	6.8451	6.1204	5.7181
	0.8	10.0410	9.2450	8.3640	7.3937	6.8537
	1	11.9517	11.0266	9.9715	8.7531	8.0737
100	0	5.0576	4.5580	4.1445	3.9300	3.8059
	0.2	5.5142	4.9922	4.5346	4.2393	4.0724
	0.4	6.6996	6.1123	5.5422	5.0548	4.7835
	0.6	8.3074	7.6215	6.9019	6.1789	5.7771
	0.8	10.1382	9.3326	8.4450	7.4736	6.9326
	1	12.0908	11.1528	10.0874	8.8641	8.1815

series so that the boundary conditions of the plate (Eqs. 29) are satisfied.

Using Eqs. (31), a homogenous system of equations is obtained. Solving the resulted characteristic equation leads to determining the natural frequencies.

3 Numerical Results and Discussions

In order to validate the results, a comparison is made with the available results in the literature. Hence, consider a simply supported micro-plate made of epoxy with the following properties (Reddy 2011):

$$E = 14.4\ \text{GPa}, \rho = 1220\ \text{kg/m}^3, v = 0.3, l = 17.6 \times 10^{-6}\ \text{m} \tag{32}$$

In Tables 1 and 2, dimensionless natural frequency $\bar{\omega} = \omega \frac{l_1^2}{h}\sqrt{\frac{\rho}{E}}$ of simply supported homogeneous square micro-plate is compared with the shown natural frequencies by Yin et al. (2010) (based on classical plate theory (CPT)) and by Thai and Kim (2013) (based on third-order shear deformable plate theory (TSDT)), respectively. Also, in Table 3 the non-dimensional natural frequencies $\tilde{\omega} = \omega h\sqrt{\frac{\rho_c}{E_c}}$ obtained from HOSNDPT and the results based on the TSDT (Thai and Kim 2013) are compared, while the order of Legendre polynomial is 5. According to these tables, it is clear that there is a good agreement between the presented results and those shown in the literature.

In order to have a numerical study, it is assumed that FG micro-plate is made of alumina and aluminum with the following material properties (Salamat-Talab et al. 2012):

$$E_m = 70\ \text{GPa}, \rho_m = 2702\ \text{kg/m}^3, E_c = 380\ \text{GPa}, \rho_c = 3800\ \text{kg/m}^3, v = 0.3 \tag{33}$$

Also, the material length scale parameter is 17.6×10^{-6} m (Lam et al. 2003). In Table 4, the convergence of results versus different orders of Legendre polynomial is tabulated. Based on the table, it is clear that for thin micro-plates results converge for small values of k, but for thick micro-plates, they converge for bigger values

Table 6 Dimensionless natural frequency $\bar{\omega}$ for rectangular homogeneous ($N = 0$) micro-plate

l_1/h	l/h	l_1/l_2				
		0.25	0.5	1	2	4
5	0	2.9654	3.4513	5.3036	11.6454	29.1609
	0.2	3.2118	3.7395	5.7561	12.7265	32.7436
	0.4	3.8435	4.4759	6.8966	15.3460	40.7161
	0.6	4.6880	5.4563	8.3932	18.6430	47.8915
	0.8	5.6267	6.5409	10.0214	22.0568	52.8013
	1	6.5932	7.6512	11.6544	24.1658	58.4783
10	0	3.1163	3.6548	5.7769	13.8050	40.7499
	0.2	3.3696	3.9524	6.2495	14.9581	44.4555
	0.4	4.0132	4.7282	7.4765	17.9037	53.5092
	0.6	4.9333	5.7850	9.1389	21.8251	65.0061
	0.8	5.9602	6.9858	11.0167	26.1635	77.0401
	1	7.0486	8.2561	12.9881	30.6046	87.4886
20	0	3.1587	3.7131	5.9219	14.6194	47.4461
	0.2	3.4142	4.0135	6.4016	15.8094	51.3882
	0.4	4.0848	4.8018	7.6587	18.9130	61.4966
	0.6	5.0047	5.8828	9.3801	23.1398	75.0082
	0.8	6.0594	7.1215	11.3494	27.9433	90.0274
	1	7.1873	8.4456	13.4498	33.0245	105.4909

of k; thus, in the following, fifth-order theory of HOSNDPT is used.

In Tables 5, 6 and 7, non-dimensional natural frequencies are presented where variations of different parameters are considered. Based on the tables, it is clear that considering material length scale parameter leads to increasing the stiffness of micro-plate; therefore, dimensionless natural frequencies increase as the material length scale parameter increases. Also, it is inferred that increasing the power law index, N, leads to decreasing the dimensionless natural frequencies. According to the tables, aspect ratio of the micro-plate, l_1/l_2, affects the responses. As shown in Table 7, the natural frequency is influenced by the side-to-thickness ratio (l_1/h).

Figure 2 shows the effect of the material length scale parameter l on dimensionless natural frequency $\bar{\omega}$ of a square micro-plate. According to this figure, increasing the material length scale parameter increases the dimensionless natural frequency. Also, as the length of micro-plate increases, the dimensionless natural frequency increases. According to this figure, variation of results is more apparent for plates with thickness near to the material length scale parameter.

The effect of material properties on dimensionless natural frequency $\bar{\omega}$ of a square FG micro-plate is depicted in Fig. 3. Based on the figure, increasing the power law index

Table 7 Dimensionless natural frequency $\bar{\omega}$ for rectangular FG micro-plate

N	l_1/h	l/h	l_1/l_2				
			0.25	0.5	1	2	4
1	5	0	2.2801	2.6566	4.0989	9.1072	23.3310
		0.2	2.5025	2.9169	4.5078	10.0835	26.4963
		0.4	3.0637	3.5715	5.5234	12.4176	33.3879
		0.6	3.7996	4.4264	6.8307	15.2959	39.8118
		0.8	4.6065	5.3592	8.2330	18.2260	43.9179
		1	5.4302	6.3058	9.6264	20.0798	48.5757
	20	0	2.4123	2.8359	4.5246	11.1853	36.4816
		0.2	2.6424	3.1065	4.9566	12.2578	40.0399
		0.4	3.2351	3.8033	6.0682	15.0054	49.0196
		0.6	4.0322	4.7400	7.5606	18.6746	60.7938
		0.8	4.9339	5.7992	9.2450	22.7888	73.7044
		1	5.8902	6.9219	11.0266	27.1047	86.8823
5	5	0	1.9218	2.2319	3.4047	7.3433	18.0000
		0.2	2.0860	2.4252	3.7141	8.1213	20.6906
		0.4	2.4998	2.9087	4.4700	9.8927	25.9052
		0.6	3.0477	3.5453	5.4444	12.0412	30.3257
		0.8	3.6552	4.2473	6.4982	14.2358	33.4590
		1	4.2804	4.9654	7.5536	15.5970	36.9570
	20	0	2.0766	2.4406	3.8893	9.5718	30.7483
		0.2	2.2410	2.6339	4.1986	10.3450	33.3768
		0.4	2.6728	3.1417	5.0090	12.3528	39.9970
		0.6	3.2665	3.8393	6.1204	15.0847	48.7638
		0.8	3.9484	4.6403	7.3937	18.1910	58.4833
		1	4.6785	5.4973	8.7531	21.4792	68.4858

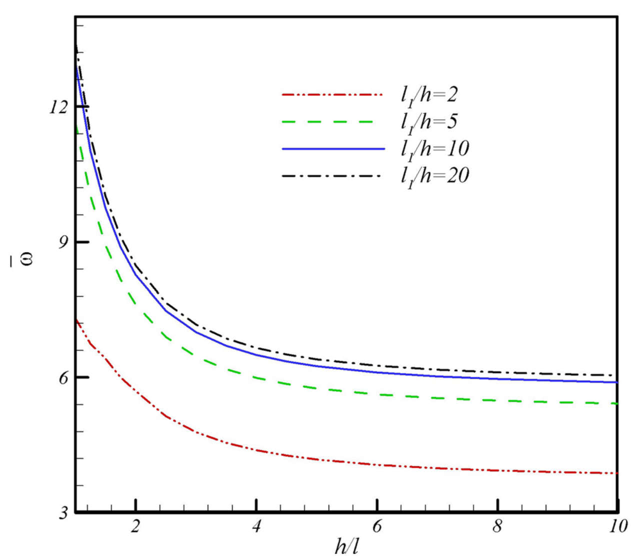

Fig. 2 Effect of the material length scale parameter l on dimensionless natural frequency $\bar{\omega}$ for a square micro-plate

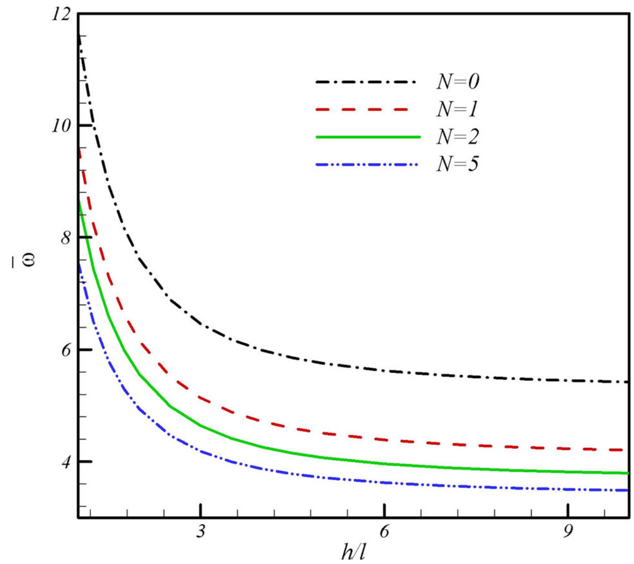

Fig. 3 Effect of the material properties on the dimensionless natural frequency $\bar{\omega}$ of a square FG micro-plate

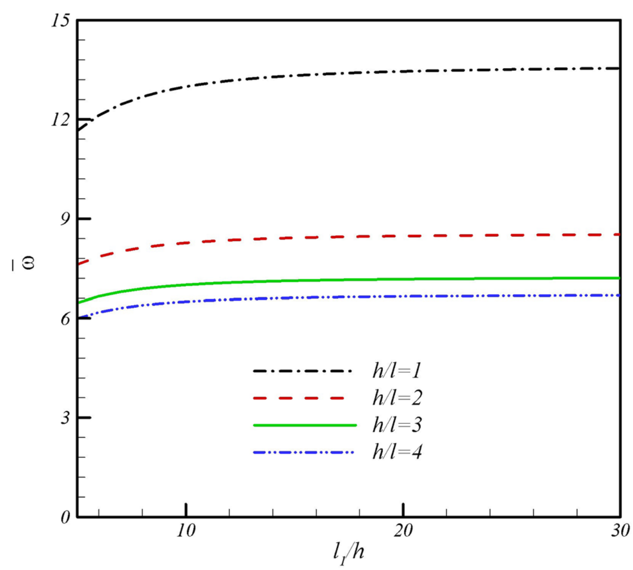

Fig. 4 Effect of the thickness ratio l_1/h on the dimensionless natural frequency $\bar{\omega}$ of a square micro-plate

reduces the dimensionless natural frequency of FG micro-plate. Also, changes in dimensionless natural frequencies are more considerable for micro-plates with thickness/material length scale ratio less than 3.

Figure 4 shows the effect of the length-to-thickness ratio on dimensionless natural frequency $\bar{\omega}$ of a square micro-plate. According to this figure, variation of natural frequencies is more apparent for smaller values of length-to-thickness ratio.

4 Conclusions

In the present paper, free vibration analysis of thick functionally graded micro-plates was investigated. Higher-order shear and normal deformable plate theory in conjunction with modified couple stress theory with one length scale parameter was used. Comparing the results with the available results in the literature shows that the presented model and solution have good agreement with the other results. An analytical solution for free vibration of simply supported FG micro-plate was presented. According to the numerical results, it is inferred that the inclusion of micro-structures affects the micro-plate behavior so that the equivalent flexural rigidity increases. Thus, modeling micro-plates with classical plate theories leads to inaccurate results. Also, it is seen that increasing the material length scale parameter increases the non-dimensional natural frequencies. In addition, increasing the power law index reduces the dimensionless natural frequencies. Numerical study indicates that while the thickness of micro-plate is the same as the material length scale parameter, variation of result is more apparent. This change in results vanishes as the ratio of thickness to material length scale parameter increases. As depicted in figures, increasing the aspect ratio increases the dimensionless natural frequencies.

References

Akgöz B, Civalek Ö (2011) Strain gradient elasticity and modified couple stress models for buckling analysis of axially loaded micro-scaled beams. Int J Eng Sci 49:1268–1280

Akgöz B, Civalek Ö (2012) Free vibration analysis for single-layered graphene sheets in an elastic matrix via modified couple stress theory. Mater Des 42:164–171

Akgöz B, Civalek Ö (2015) A microstructure-dependent sinusoidal plate model based on the strain gradient elasticity theory. Acta Mech 226:2277–2294

Akgöz B, Civalek Ö (2017) Effects of thermal and shear deformation on vibration response of functionally graded thick composite microbeams. Compos B Eng 129:77–87

Arbind A, Reddy JN, Srinivasa AR (2014) Modified couple stress-based third-order theory for nonlinear analysis of functionally graded beams. Latin Am J Solids Struct 11:459–487

Asghari M, Taati E (2013) A size-dependent model for functionally graded micro-plates for mechanical analyses. J Vib Control 19:1614–1632

Asghari M, Kahrobaiyan MH, Ahmadian MT (2010) A nonlinear Timoshenko beam formulation based on the modified couple stress theory. Int J Eng Sci 48:1749–1761

Batra RC, Vidoli S (2002) Higher order piezoelectric plate theory derived from a three-dimensional variational principle. AIAA J 40:91–104

Chong ACM, Yang F, Lam DCC, Tong P (2001) Torsion and bending of micron-scaled structures. J Mater Res 16:1052–1058

Eringen AC (1967) Theory of micropolar plates. Z Angew Math Phys 18:12–30

Eringen AC (1972) Nonlocal polar elastic continua. Int J Eng Sci 10:1–16

Eshraghi I, Dag S, Soltani N (2016) Bending and free vibrations of functionally graded annular and circular micro-plates under thermal loading. Compos Struct 137:196–207

Fu Y, Du H, Zhang S (2003) Functionally graded TiN/TiNi shape memory alloy films. Mater Lett 57:2995–2999

Ghayesh MH, Farokhi H, Gholipour A (2017) Vibration analysis of geometrically imperfect three-layered shear-deformable microbeams. Int J Mech Sci 122:370–383

Gurtin ME, Weissmuller J, Larche F (1998) A general theory of curved deformable interfaces in solids at equilibrium. Philos Mag A 78:1093–1109

Jomehzadeh E, Noori HR, Saidi AR (2011) The size-dependent vibration analysis of micro plates based on a modified couple stress theory. Physica E 43:877–883

Kahrobaiyan MH, Asghari M, Rahaeifard M, Ahmadian MT (2010) Investigation of the size-dependent dynamic characteristics of atomic force microscope micro-cantilevers based on the modified couple stress theory. Int J Eng Sci 48:1985–1994

Ke LL, Wang YS (2011) Size effect on dynamic stability of functionally graded micro-beams based on a modified couple stress theory. Compos Struct 93:342–350

Ke LL, Wang YS, Yang J, Kitipornchai S (2012) Free vibration of size-dependent Mindlin microplates based on the modified couple stress theory. J Sound Vib 331:94–106

Koiter WT (1964) Couple stresses in the theory of elasticity, I and II. Nederl Akad Wetensch Proc Ser B 67:17–29

Kong S, Zhou S, Nie Z, Wang K (2008) The size-dependent natural frequency of Bernoulli–Euler micro-beams. Int J Eng Sci 46:427–437

Lam DCC, Yang F, Chong ACM, Wang J, Tong P (2003) Experiments and theory in strain gradient elasticity. J Mech Phys Solids 51:1477–1508

Lee Z, Ophus C, Fischer L, Nelson-Fitzpatrick N, Westra KL, Evoy S et al (2006) Metallic NEMS components fabricated from nanocomposite Al–Mo films. Nanotechnology 17:3063–3070

Lu C, Wu D, Chen W (2011) Non-linear responses of nano-scale FGM films including the effects of surface energies. IEEE Trans Nanotechnol 10(6):1321–1327

Ma HM, Gao XL, Reddy JN (2008) A microstructure-dependent Timoshenko beam model based on a modified couple stress theory. J Mech Phys Solids 56:3379–3391

Ma HM, Gao XL, Reddy JN (2011) A non-classical Mindlin plate model based on a modified couple stress theory. Acta Mech 220:217–235

Mindlin RD, Tiersten HF (1962) Effects of couple-stresses in linear elasticity. Arch Ration Mech Anal 11:415–448

Mohseni E, Saidi AR, Mohammadi M (2017) Bending-stretching analysis of thick functionally graded micro-plates using higher-order shear and normal deformable plate theory. Mech Adv Mater Struct 24:1221–1230

Park SK, Gao X-L (2006) Bernoulli–Euler beam model based on a modified couple stress theory. J Micromech Microeng 16:2355–2359

Rahaeifard M, Kahrobaiyan MH, Ahmadian MT (2009) Sensitivity analysis of atomic force microscope cantilever made of functionally graded materials. In: 3rd International conference on micro- and nano-systems. ASME power transmission and gearing conference, pp 539–544

Reddy JN (2002) Energy principles and variational methods in applied mechanics. Wiley, New York

Reddy JN (2011) Microstructure-dependent couple stress theories of functionally graded beams. J Mech Phys Solids 59:2382–2399

Reddy JN, Kim J (2012) A nonlinear modified couple stress-based third-order theory of functionally graded plates. Compos Struct 94:1128–1143

Roque CMC, Ferreira AJM, Reddy JN (2013) Analysis of Mindlin micro plates with a modified couple stress theory and a meshless method. Appl Math Model 37:4626–4633

Salamat-Talab M, Nateghi A, Torabi J (2012) Static and dynamic analysis of third-order shear deformation FG micro beam based on modified couple stress theory. Int J Mech Sci 57:63–73

Sheikholeslami SA, Saidi AR (2013) Vibration analysis of functionally graded rectangular plates resting on elastic foundation using higher-order shear and normal deformable plate theory. Compos Struct 106:350–361

Thai HT, Kim SE (2013) A size dependent functionally graded Reddy plate model based on a modified couple stress theory. Compos Part B Eng 45:1636–1645

Thai HT, Vo T (2013) A size-dependent functionally graded sinusoidal plate model based on a modified couple stress theory. Compos Struct 96:376–383

Toupin RA (1962) Elastic materials with couple-stresses. Arch Ration Mech Anal 11:385–414

Tsiatas GC (2009) A new Kirchhoff plate model based on a modified couple stress theory. Int J Solids Struct 46:2757–2764

Witvrouw A, Mehta A (2005) The use of functionally graded poly-SiGe layers for MEMS applications. Mater Sci Forum 492–493:255–260

Xiao JR, Gilhooley DF, Batra RC, Gillespie JW Jr, McCarthy MA (2008) Analysis of thick composite laminates using a higher-order shear and normal deformable plate theory (HOSNDPT) and a meshless method. Compos Part B 39:414–427

Yang F, Chong ACM, Lam DCC, Tong P (2002) Couple stress based strain gradient theory for elasticity. Int J Solids Struct 39:2731–2743

Yin L, Qian Q, Wang L, Xia W (2010) Vibration analysis of microscale plates based on modified couple stress theory. Acta Mech Solida Sin 23:386–393